

# Separation of close-boiling hydrocarbon mixtures by MFI and FAU membranes made by secondary growth

Sankar Nair, Zhiping Lai, Vladimiro Nikolakis, George Xomeritakis,  
Griselda Bonilla, Michael Tsapatsis \*

*Department of Chemical Engineering, 159 Goessmann Laboratory, University of Massachusetts Amherst, Amherst, MA 01003 3110, USA*

Received 6 August 2000; received in revised form 17 January 2001; accepted 17 January 2001

## Abstract

We summarize and discuss recent results on the separation of close-boiling hydrocarbon mixtures by means of zeolite membranes. We focus on the separation of xylene isomers using silicalite (MFI) membranes, as well as several other hydrocarbon mixtures using faujasite membranes. In the case of the silicalite membranes, the selectivity is found to depend on the membrane microstructure. Permeation of xylene isomers through the silicalite membranes occurs through both zeolitic and non-zeolitic (intercrystalline) nanopores. This hypothesis is supported by vapor-phase permeation results on silicalite membranes synthesized with different microstructures, and by confocal microscopy experiments. In addition, a simple method for repairing calcination-induced membrane defects is presented, and its application is found to be essential in obtaining high (20–300) *p*-xylene/*o*-xylene separation factors. The faujasite membranes are found to have high selectivities (40–150) in the separation of binary mixtures containing one aromatic component, and modest selectivities (4–9) for the separation of unsaturated from saturated low-molecular-weight hydrocarbons. © 2001 Elsevier Science B.V. All rights reserved.

*Keywords:* Membrane; Xylene; Permeation; Faujasite; Grain boundaries

## 1. Introduction

Zeolite membrane-based separations have generated much interest in recent years. They are attractive for a variety of reasons, including steady-state operation, tailored selectivity, low energy consumption, and potential for combined reaction-separation systems. Several zeolites are known to separate organic molecules based on their properties of preferential adsorption, preferential dif-

fusion, or pure molecular sieving (size exclusion) [1]. Among these, the MFI [2] structure (i.e., silicalite or its aluminosilicate analog, ZSM-5) has been often employed in laboratory membrane devices. Owing to its medium-size ( $\sim 6$  Å) pore network, it is capable, in principle, of effecting separations of many industrially important hydrocarbon species. Furthermore, its synthetic chemistry is well established in the literature. Faujasite is another zeolite that has been extensively used in industry. It has larger pores ( $\sim 7.4$  Å) [2] than silicalite, hence it can be used in applications involving larger molecules compared to those that can be accommodated in medium-pore

\* Corresponding author. Tel.: +1-413-545-0276; fax: +1-413-545-1647.

*E-mail address:* tsapatsis@ecs.umass.edu (M. Tsapatsis).

zeolites. Furthermore, modification of the faujasite crystals, either by ion exchange or de-alumination, can be used to control the adsorption or intracrystalline diffusion properties, providing a method of tailoring the membranes to specific applications.

Several methods have been used to synthesize zeolitic membranes. The earliest attempts involved impregnation of zeolite crystals in polymer matrices [3]. Free-standing zeolite membranes have also been prepared but are of limited use because of their poor mechanical durability [4]. Asymmetric (supported) silicalite membranes have been synthesized mainly by the *in situ* method of hydrothermal synthesis [5]. This method involves exposure of the support surface to a hydrothermal growth solution, resulting in nucleation and subsequent growth of zeolite crystals on the surface to form a continuous membrane. A second method that enables better control and flexibility, is that of secondary (seeded) growth [6–8]. In this method, nucleation is decoupled from crystal growth by pre-deposition of a seed layer of zeolite crystals ( $\approx 50$  nm in size) from a colloidal suspension onto the support. The seed layer is then hydrothermally grown into a continuous membrane. This method is used to synthesize the membranes considered in this report. Silicalite and ZSM-5 membranes synthesized by either method, have been found to possess good gas-phase hydrocarbon separation characteristics [9–11]. Synthesis of faujasite (Na–Y or Na–X) membranes on porous  $\alpha$ -alumina supports has also been demonstrated in the literature [12–15], by using either direct (*in situ*) or secondary growth methods. They have been successfully used for the separation of  $\text{CO}_2/\text{N}_2$ ,  $\text{CH}_4/\text{H}_2$ ,  $\text{C}_2\text{H}_6/\text{H}_2$ ,  $\text{C}_3\text{H}_8/\text{H}_2$ , and  $\text{CO}_2/\text{H}_2$  gas mixtures [16,17]. They have also been used to separate methanol/methyl tert-butyl ether [15] and water/ethanol [13] liquid mixtures through pervaporation.

The separation of xylene isomers is of considerable importance in the petrochemical industry. The separation is difficult because of the close boiling points of the isomers. The difference in their kinetic diameters ( $\approx 5.8$  Å for *p*-xylene and  $\approx 6.8$  Å for *o*- and *m*-xylene) indicates the possibility of effective separation using silicalite membranes. However, the performance of silicalite

membranes during binary permeation of xylene isomers is generally poor [7,11,18]. In an earlier publication [11], we have discussed the xylene–silicalite system in some detail, concentrating mainly on the flexibility and phase transitions of the silicalite structure upon adsorption of close-fitting molecules like the xylene isomers. In this paper, we further investigate the permeation mechanism of xylene isomers in silicalite membranes. It is shown that the permeation characteristics of an apparently dense, well-intergrown silicalite membrane, is nevertheless strongly affected by the intergrain porosity. This intergrain porosity is different from that created by membrane defects (such as pinholes and cracks), and is an unavoidable result of the synthesis conditions. Thin silicalite membranes (2–3  $\mu\text{m}$  in thickness) grown at a lower synthesis temperature are prone to cracking upon calcination. These have a different microstructure from the thick membranes described previously, with more well-intergrown crystals. In this case, we show that the cracks can be repaired by coating a thick silica or silica–surfactant layer over the zeolite membrane. This layer peels off easily from the membrane surface but remains in the interior of the pre-existing cracks. The thin, repaired membranes so obtained are found to be selective for *p*-xylene over *o*-xylene. Further, we have used confocal microscopy [19–21] to obtain information regarding the microstructure of both thick and thin silicalite membranes. The results support the hypotheses made in this work, regarding the permeation characteristics of silicalite membranes made by secondary growth.

We have also recently reported a method for synthesizing faujasite Na–X membranes on alumina supports by using *in situ* and secondary (seeded) growth techniques [22]. In the same report the ability of the membranes to separate unsaturated from saturated hydrocarbons has been illustrated by considering a variety of gas or vapor hydrocarbon mixtures, such as benzene/cyclohexane, benzene/*n*-hexane, toluene/*n*-heptane, propylene/propane, and ethylene/methane. The benzene/cyclohexane separation has been studied in more detail, since it is a close boiling point system over all ranges of composition and therefore is a challenging [23] separation. The processes (azeotropic

or extractive distillation) currently used in industry to separate these mixtures are limited by the vapor–liquid equilibrium and are practical over a narrow range of feed compositions. Propane/propylene is another close-boiling mixture the separation of which is also difficult to achieve by distillation [24]. Even though a hybrid distillation/membrane system has been proposed to enhance the separation and reduce the height of the distillation column, such a set up cannot be built due to the lack of a commercial membrane that has high enough selectivity for this type of mixtures [24]. The preparation of a highly selective membrane will improve the economics of the separation by operating a hybrid process in place of the distillation column. In the present report the temperature effect on the separation behavior on the hydrocarbon mixtures mentioned above has been examined.

## 2. Experimental

### 2.1. MFI (silicalite) membrane synthesis

Silicalite membranes were synthesized using the secondary (seeded) growth method, as described in our earlier publications. An aqueous suspension of  $\approx 80$ -nm-silicalite crystals ( $\sim 5$  g/l) was first used to deposit a precursor layer onto a polished  $\alpha$ -alumina support. Two types (A and B) of MFI membranes were subsequently synthesized by secondary growth methods. Type A membranes were synthesized with a hydrothermal reaction mixture of composition  $4\text{SiO}_2:0.9\text{KOH}:0.9\text{TPABr}$  (tetrapropylammonium bromide): $950\text{H}_2\text{O}:16\text{EtOH}$  [11]. The synthesis was carried out at  $175^\circ\text{C}$  for a period of 24 h. Synthesis of Type B membranes proceeded from a reaction solution of the same composition, but at a temperature of  $90^\circ\text{C}$  for a period of 120 h. The membranes are then rinsed in deionized water and calcined at  $525^\circ\text{C}$  for 5 h (Type A), or at  $450^\circ\text{C}$  for 6 h (Type B).

### 2.2. Microcrack sealing in Type B membranes

The Type B membranes, after calcination, are dip coated with a surfactant-templated silica sol

[25] to add a mesostructured surfactant–silica layer, which can be easily removed from the membrane surface using compressed air. The cracks in the membrane are plugged by infiltration of the silica–surfactant composite during coating. More details regarding this procedure are given in Ref. [26]. Alternatively, we report here that the cracks can be plugged using a silica sol–gel coating in the absence of surfactant.

### 2.3. FAU membrane synthesis

Faujasite membranes were prepared on porous  $\alpha$ -alumina supports by using the secondary growth method. An aqueous suspension of ZSM-2 nanocrystals (particle size  $\sim 200$  nm, 10 g/l, pH  $\sim 8$ ) was first prepared from a mixture having molar composition [27]  $0.53\text{Li}_2\text{O}:1\text{Al}_2\text{O}_3:6\text{TMAOH}$  (tetramethylammonium hydroxide): $3.4\text{SiO}_2:315\text{H}_2\text{O}$  that was hydrothermally treated at  $140^\circ\text{C}$  for 12 h. The seeds were then deposited on the alumina supports following the procedure described elsewhere [6,11]. The seeded supports were then placed in Teflon-lined stainless steel autoclaves and were hydrothermally treated at  $85^\circ\text{C}$  with a mixture of molar composition  $4.17\text{Na}_2\text{O}:1.0\text{Al}_2\text{O}_3:10\text{TEA}$  (triethanol ammonium): $1.87\text{SiO}_2:460\text{H}_2\text{O}$ . This molar composition is known [28] to result in nucleation and growth of Na–X faujasite crystals. The silica and alumina sources were tetraethylorthosilicate (TEOS, 98%, Aldrich) and aluminum foil (Al 99.8%, 0.05 mm thick, Aldrich) respectively. After hydrothermal growth, the membranes were cooled, washed several times with distilled water and then heat treated in air at  $450^\circ\text{C}$  for 5 h, to remove any TEA from the zeolite pores. Further details of the membrane preparation and characterization can be found in Ref. [22].

### 2.4. Permeation experiments

Vapor-phase permeation experiments were carried out in the Wicke–Kallenbach mode using a modified version of a setup described previously [11,26]. Helium streams are passed through heated bubblers containing individual condensible organic components, and then mixed (with the possible addition of a diluent helium stream) to create

a feedstream of the desired composition. The temperature of the bubblers is maintained within an accuracy of  $\pm 1^\circ\text{C}$ . All flow streams are heated to prevent condensation of the organic vapors. The permeate side of the membrane is flushed with a helium sweep, which is then analyzed by a gas chromatograph. Mass flow controllers are used to control the flow rates of all streams. The apparatus is also easily adapted for gas permeation experiments.

### 2.5. Confocal microscopy

The MFI membranes were impregnated with a fluorescent dye, fluorescein-Na salt, and fixed on glass slides. A Bio-Rad MRC-600/1000 unit equipped with an Ar-Kr laser with 488, 508, and 647 nm wavelengths and an oil-immersion objective lens with a numerical aperture of 0.85 was used to obtain the confocal images. More details can be found in Ref. [19].

## 3. Results and discussion

### 3.1. Membrane characterization

Type A silicalite membranes are approximately 15  $\mu\text{m}$  thick (measured by SEM), exhibit *c*-out-of-plane orientation (as confirmed from X-ray diffraction), and have a columnar microstructure with (1 0 1) facets visible at an angle to the surface. Type B membranes are approximately 1–3  $\mu\text{m}$  thick and are (1 0 1) oriented with a smooth surface. Type B membranes develop cracks upon calcination, which are subsequently repaired as described in the experimental section. Fig. 1 shows a 1  $\mu\text{m}$  thick Type B membrane. Fig. 1a shows a cross-sectional view of the as-synthesized membrane, whereas Fig. 1b shows a top view of a membrane whose calcination-induced cracks have been sealed with silica (applied in the absence of surfactant).

The ZSM-2 seeds are hexagonal plate-like crystals of  $\sim 250$  nm which fully cover the surface of the support. SEM top-view images show that after  $\sim 21$  days of growth, a continuous well-intergrown crystalline layer is formed. The film

thickness, as calculated from the SEM cross-section, is about 30  $\mu\text{m}$  after  $\sim 21$  days of hydrothermal treatment, and mainly consists of intergrown large grains. The Si/Al ratio over the entire cross-section of the membrane was estimated with microprobe analysis, and found to be in the range of 1–1.5, which is characteristic of the Na-X form of faujasite [2].

### 3.2. Permeation of xylene isomers through Type A silicalite membranes

Fig. 2 shows single-component and binary permeation data for Type A silicalite membranes, as a function of feed partial pressure. Three flux isotherms are measured at three different temperatures. The pressure (*x*-axis) in each case is normalized by the saturation vapor pressure ( $p_{\text{sat}}$ ) of the component in question, at each temperature that was studied. The membranes were previously tested for defects and quality using the butane isomers. Binary selectivities greater than 40 (for *n*-butane over *i*-butane from a 50:50 mixture of the two isomers) are obtained, indicating that the membranes are of good quality. Fig. 2a shows the single-component flux of *p*-xylene. It is clear that the single-component flux of *p*-xylene does not saturate as the feed partial pressure is increased. Furthermore, the flux appears to increase sharply at higher partial pressures. However, the single-component permeation behavior of *o*-xylene is somewhat different (Fig. 2b). In this case, the flux saturates at moderate partial pressures, but then increases sharply at higher partial pressures. From Fig. 2a and b, it is apparent that the *o*-xylene flux is between one and two orders of magnitude lower than the *p*-xylene flux. The single-component selectivities are therefore quite high, especially at moderate feed pressures. A selectivity of about 100 is obtained at  $50^\circ\text{C}$ , with  $p/p_{\text{sat}} \sim 0.6$ . The selectivity decreases with increasing temperature, and shows a maximum as a function of partial pressure.

The observed behavior of the *p*-xylene flux as a function of partial pressure suggests that the grain boundaries play a substantial role in transport of *p*-xylene through the membrane. It appears that *p*-xylene molecules can gain increasing access to the

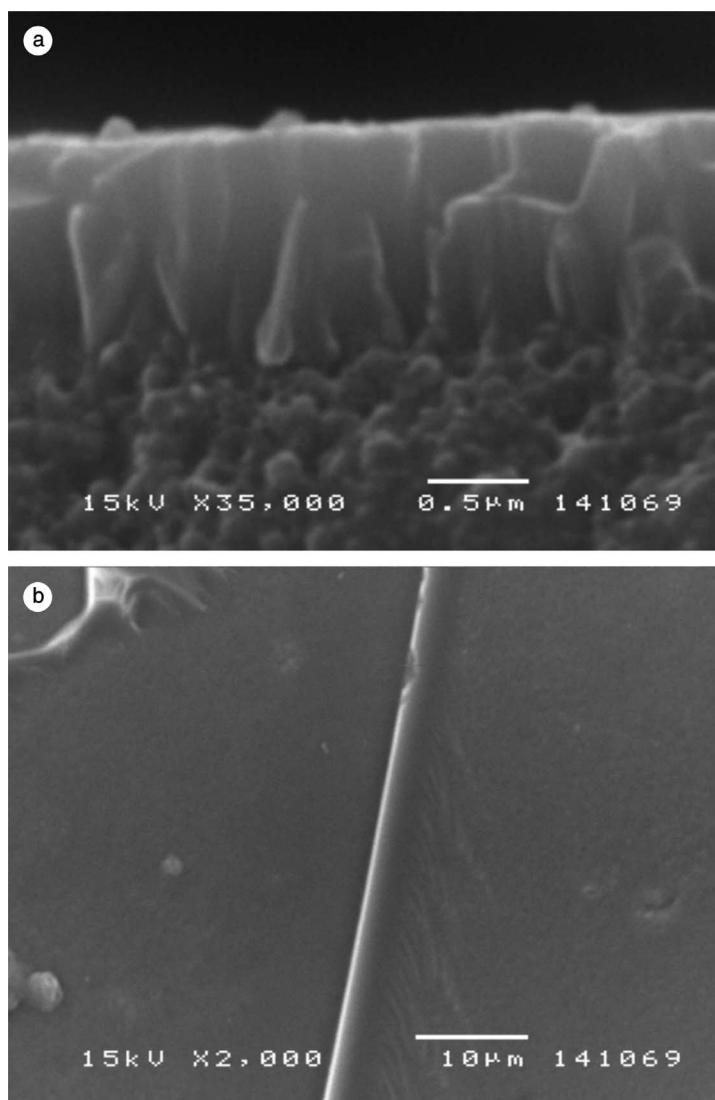


Fig. 1. SEM images of (a) cross-section of Type B MFI membrane, (b) top view of Type B MFI membrane showing a crack sealed with silica.

intergrain porosity as the *p*-xylene concentration in the feed increases. At present, we do not completely understand the reasons for this type of pressure dependence. However, a plausible explanation can be advanced. It is hypothesized that the adsorption of *p*-xylene molecules can lead to progressive “opening” of the intercrystalline grain boundaries. On the other hand, *o*-xylene adsorbs less and diffuses very slowly in silicalite, and is not

able to generate sufficient deformation in the membrane. Notwithstanding the reason for the different permeation characteristics of the two isomers in the low to moderate partial pressure range, it seems clear that the abrupt increase in the single-component flux of both isomers in the high-pressure region, is due to a capillary condensation type phenomenon occurring in the intercrystalline nanopores of the membrane. Thus, it is suspected

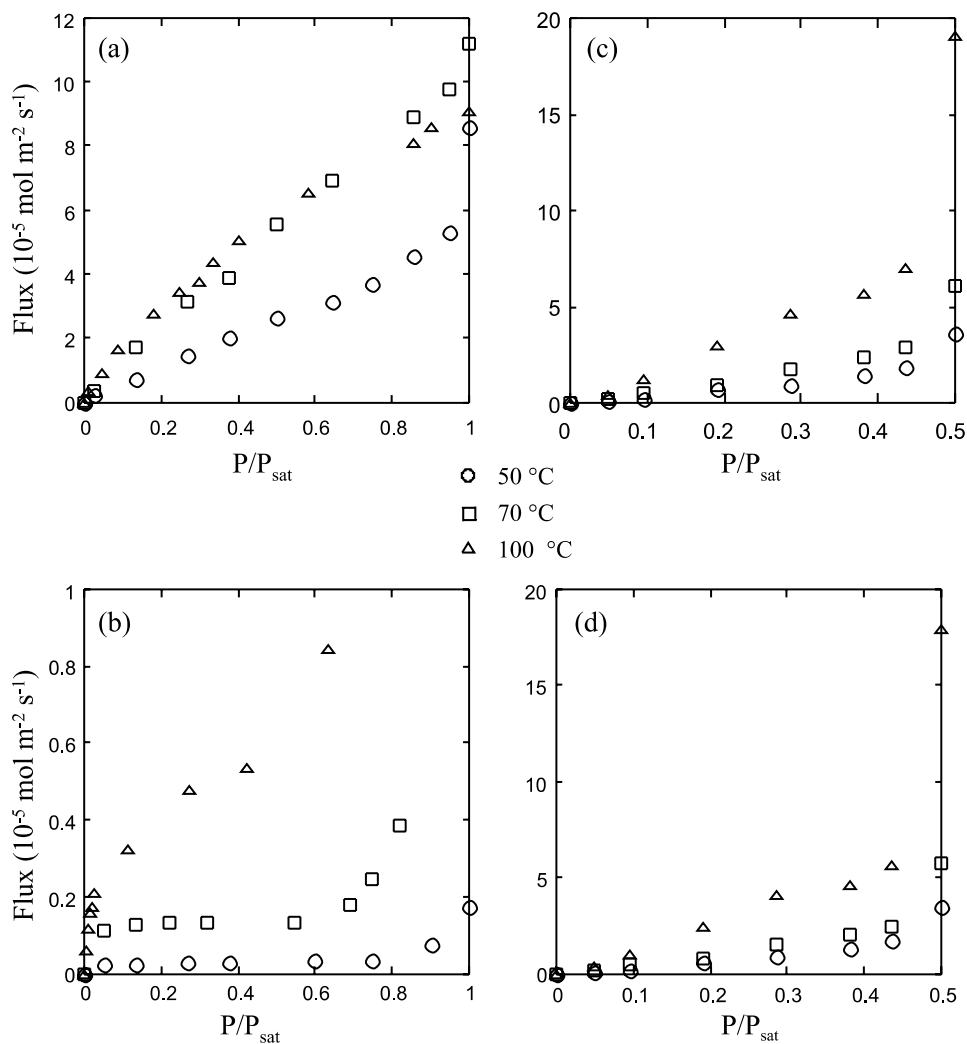


Fig. 2. Permeation fluxes through Type A MFI membrane at different temperatures: (a) single-component *p*-xylene, (b) single-component *o*-xylene, (c) binary *p*-xylene, and (d) binary *o*-xylene.

that the adsorption–diffusion characteristics of the two isomers in the grain boundaries (which may be modeled as slit nanopores) have a role in determining the permeation behavior observed above. The binary permeation data for a Type A silicalite membrane is presented in Fig. 2c and d. It is apparent that the membrane is not selective for *p*-xylene. In this case, the behavior of the *p*-xylene flux does not deviate significantly from the single-component case. However, the *o*-xylene flux is dramatically enhanced by the presence of *p*-xylene

and is of the same order of magnitude as the *p*-xylene flux. We have reported this effect in earlier work [11,26]. This behavior is consistent with the mechanism proposed above, since in the case of binary permeation, *o*-xylene would have easier access to the grain boundary regions, which are opened up by the presence of *p*-xylene. As in the case of single-component permeation, there is a rapid increase of the binary fluxes in the high-pressure region, which is due to a capillary condensation mechanism operating in the inter-

crystalline nanopores. These results are in agreement with those of our confocal microscopy experiments, described in Section 3.4.

### 3.3. Separation of xylene isomers with Type B silicalite membranes

From the above results, it appears that Type A membranes may not be suitable for separation of xylene isomers. Hence, Type B membranes were developed as described earlier. Table 1 shows binary permeation data for several Type B samples after microcrack sealing. Preliminary measurements showed that the selectivity reaches a maximum at 125°C, dropping significantly at both higher and lower temperatures. The measurements of Table 1 are therefore made at this temperature. The feed is a 50:50 mixture obtained from helium streams saturated with *p*- and *o*-xylene at room temperature. The results of Table 1 shows that high selectivities (20–300) can be obtained when the microcracks are sealed. Grain boundary effects appear to be minimal in this case, since the membranes are very well intergrown. Samples B1–B5 are repaired using a silica–surfactant sol, and their permeation behavior is reported in Ref. [26]. These data are listed for comparison with samples B6–B8, which are repaired using a silica sol in the absence of surfactant. These samples are also have

high selectivity for *p*-xylene. The selectivity remains high even after long operation times, as indicated in Table 1 for samples B7 and B8, which remained selective as long as 200 h. The flux however, falls slowly and reaches a lower limit as reported for some of the samples shown in Table 1. A more detailed investigation of this effect is currently underway. Despite the fact that these membranes are thin (0.5–2 μm), the *p*-xylene fluxes through them are not significantly higher than those through the Type A membranes at similar pressures. This is possibly due to additional resistance from any remaining layer of the silica coating that may adhere to the zeolite layer even after most of it has been peeled away. A reduction in permeability of the membrane may also be caused by the relative non-availability of grain boundaries in this case.

### 3.4. Confocal microscopy

Fig. 3a shows an optical section of a Type B (thin) membrane taken at a depth of 1 μm from the membrane surface. In this image, cracks can be clearly observed as evinced by the presence and fluorescence of the dye. These cracks are observed at the substrate and propagate along the entire thickness of the membrane. For a Type A (thick) membrane (Fig. 3b), in addition to such defects, we are also able to observe the crystal grain boundaries. These grain boundaries can also be traced along the entire thickness of the membrane. From these results, it is clear that grain boundaries are avoided in Type B membranes, while they are accessible to the bulky dye molecule in the case of Type A membranes. These results are consistent with the differences in separation performance between the two types of silicalite membranes, as described in Sections 3.2 and 3.3.

### 3.5. Separations using faujasite membranes

The permeation behavior of several hydrocarbon gas or vapor mixtures has been examined over a range of temperatures (30–220°C). The permeation fluxes and the corresponding separation factors at different temperatures for toluene/heptane, benzene/*n*-hexane, benzene/cyclohexane,

Table 1  
Binary permeation data for Type B MFI membrane samples

Sample	<i>p</i> -xylene flux (μmol m <sup>-2</sup> s <sup>-1</sup> )	Selectivity ( <i>p</i> -X/ <i>o</i> -X)
B1	17.5	66
B2	7.9	278
B3	10.2	141
B4	16.1	29
B5	2.8	23
B6 <sup>a</sup>	10.9	127
B7 <sup>a,b</sup>	85.1	35
B8 <sup>a,b</sup>	35.0	64

Feed: *p*-xylene = 0.45 kPa; *o*-xylene = 0.35 kPa; *T* = 125°C.

<sup>a</sup>Cracks were sealed with a silica sol–gel coating, in the absence of surfactant.

<sup>b</sup>For sample B7, the *p*-xylene flux declines slowly to 30 μmol m<sup>-2</sup> s<sup>-1</sup> (selectivity = 20) after 200 h; whereas for B8, the flux declines to 20 μmol m<sup>-2</sup> s<sup>-1</sup> (selectivity = 87) after 200 h.

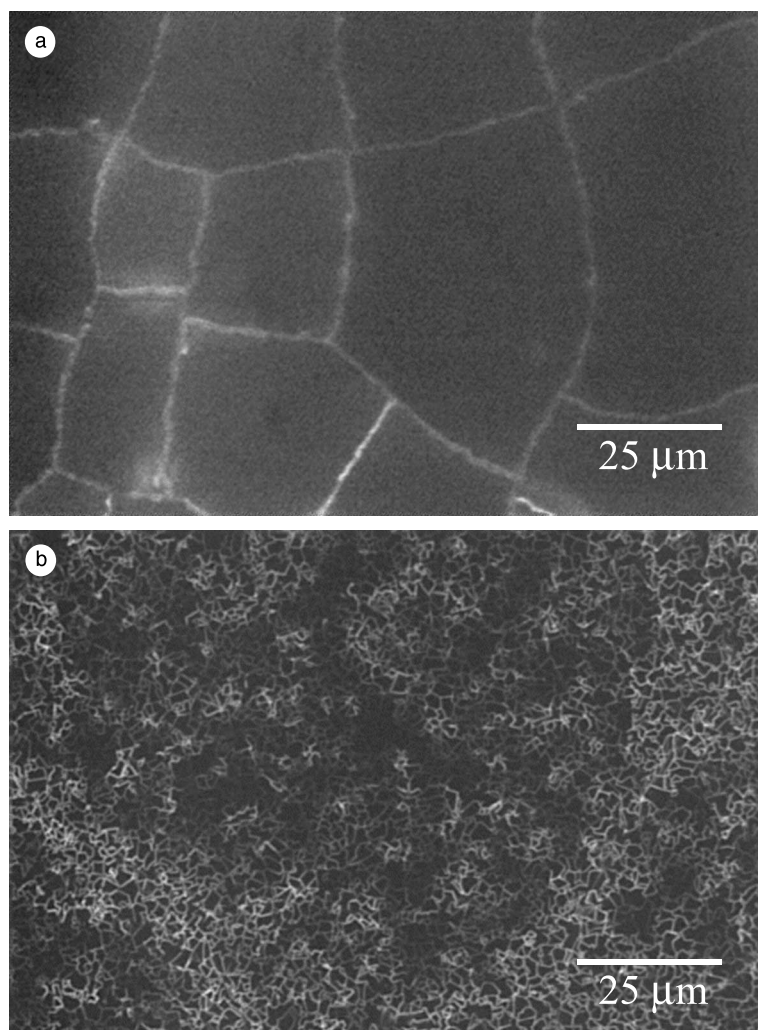


Fig. 3. Confocal microscope images of MFI membranes infiltrated with fluorescein dye: (a) Type B membrane showing cracks but no grain boundaries, and (b) Type A membranes showing grain boundaries between zeolite crystals.

ethylene/ethane, propylene/propane, and ethylene/methane equimolar feed mixtures are presented in Fig. 4. For all the mixtures examined, the membranes were permselective in favor of the unsaturated hydrocarbon. Since the size of all molecules used is smaller than the pore size of faujasite the observed separation cannot be attributed to size exclusion from the zeolite. Unsaturated hydrocarbons have stronger affinity to the cations of the zeolite resulting in stronger adsorption in the zeolite pores [29]. The separation behavior of mix-

tures containing aromatic vapors shows some differences compared with the separation of gas mixtures. In the former case the observed separation factors are much higher (40–150) and are observed at relatively high temperatures ( $>60^{\circ}\text{C}$ ). On the other hand the separation factors of the smaller hydrocarbons are smaller (4–9) and are all observed at lower temperatures ( $<40^{\circ}\text{C}$ ). This type of behavior can probably be attributed to a coupling of adsorption with intrazeolitic diffusion [22].

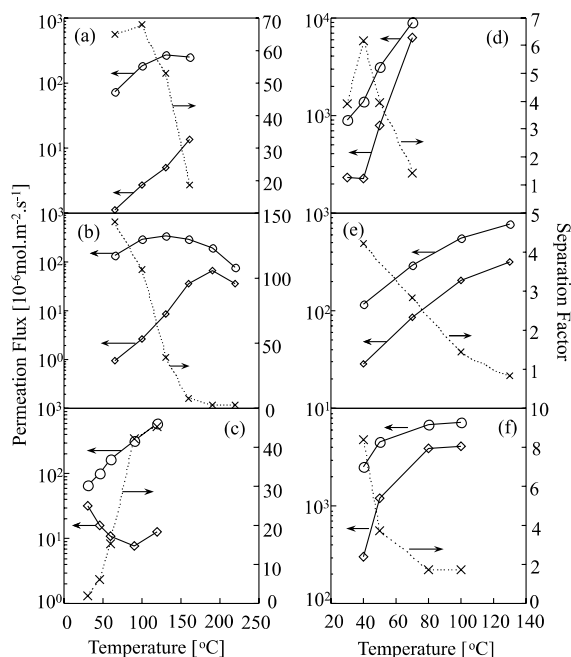


Fig. 4. Separation factors and permeation fluxes through faujasite membrane at different temperatures, for (a) 5 kPa benzene/5 kPa cyclohexane, (b) 5 kPa benzene/5 kPa *n*-hexane, (c) 5 kPa toluene/5 kPa *n*-heptane, (d) 50.5 kPa propylene/50.5 kPa propane, (e) 50.5 kPa ethylene/50.5 kPa ethane, and (f) 50.5 kPa ethylene/50.5 kPa methane binary mixtures. (○) flux of the higher-permeating hydrocarbon; (◇) flux of the lower-permeating hydrocarbon; (×) selectivity factor.

#### 4. Conclusions

The separation of close-boiling hydrocarbon mixtures by zeolite membranes has been considered. Oriented silicalite membranes have been prepared and the permeation characteristics of the xylene isomers have been measured. The dependence of the permeation characteristics on the partial pressure (upto  $\sim 20$  kPa) and temperature (upto  $125^\circ\text{C}$ ) has been investigated. Thick silicalite membranes with a columnar microstructure are found to have high single-component selectivity for *p*-xylene, but lose their selectivity in binary permeation. This is due to the enhancement of the *o*-xylene flux through the interzeolitic porosity, caused by the presence of *p*-xylene. Capillary condensation effects are also observed in these membranes when operating at higher partial pressures. On the other hand, thin silicalite membranes

grown at a lower temperature and for a longer time, and whose cracks are sealed with a silica-surfactant composite, show high selectivities for *p*-xylene. These results are found to be consistent with an examination of the membrane microstructures by confocal microscopy, confirming the role of crystal grain boundaries in determining the permeation characteristics. Faujasite membranes have also been synthesized and used for separating a variety of saturated/unsaturated hydrocarbon vapor mixtures, some of which are close boiling point systems (e.g. benzene/cyclohexane, propylene/propane). The permeation behavior has been examined over a temperature range ( $30$ – $220^\circ\text{C}$ ). The best separation factors reported, are for benzene/cyclohexane (SF = 68, at  $100^\circ\text{C}$ ), benzene/*n*-hexane (SF = 144 at  $65^\circ\text{C}$ ), toluene/*n*-heptane (SF = 45 at  $120^\circ\text{C}$ ), propylene/propane (SF = 6.2 at  $40^\circ\text{C}$ ), ethylene/ethane (SF = 4.1 at  $40^\circ\text{C}$ ), and ethylene/methane (SF = 8.4 at  $40^\circ\text{C}$ ) binary mixtures.

#### References

- [1] S. Mohanty, A.V. McCormick, Chem. Engng. J. 74 (1999) 1.
- [2] R. Szostak, Handbook of Molecular Sieves, Van Nostrand Reinhold, New York, 1992.
- [3] M. Demertzis, N.P. Evmiridis, J. Chem. Soc. Faraday Trans. 82 (1986) 3647.
- [4] Y. Kiyozumi, F. Mizukami, K. Maeda, T. Kodzasa, M. Toba, S.-I. Niwa, Prog. Zeol. Microp. Mater. 105 (1997) 2225.
- [5] J.C. Jansen, E.N. Coker, Sol. State Mater. Sci. 1 (1996) 65.
- [6] M.C. Lovallo, A. Gouzinis, M. Tsapatsis, AIChE J. 44 (1998) 1903.
- [7] H.W. Deckman, E.W. Corcoran, J.A. McHenry, W. Lai, L.R. Czarnetzki, W.E. Wales, US Patent 5,968,366, 1999.
- [8] M. Noack, P. Kolsch, J. Caro, M. Schneider, P. Toussaint, I. Sieber, Micropor. Mesopor. Mater. 35/36 (2000) 253.
- [9] Y. Yan, M.E. Davis, G. Gavalas, J. Membr. Sci. 123 (1997) 95.
- [10] K. Keizer, A.J. Burggraaf, Z.A.E.P. Vroon, H. Verweij, J. Membr. Sci. 147 (1998) 159.
- [11] G. Xomeritakis, S. Nair, M. Tsapatsis, Micropor. Mesopor. Mater. 38 (2000) 61.
- [12] K. Kusakabe, T. Kuroda, A. Murata, S. Morooka, Ind. Engng. Chem. Res. 36 (1997) 649.
- [13] I. Kumakiri, T. Yamaguchi, S. Nakao, Ind. Engng. Chem. Res. 38 (1999) 4682.
- [14] M. Lassinantti, J. Hedlund, J. Sterte, Micropor. Mesopor. Mater. 38 (2000) 25.

- [15] H. Kita, H.T. Inoue, H. Asamura, K. Tanaka, K. Okamoto, *Chem. Commun.* 15 (1997) 45.
- [16] K. Kusakabe, T. Kuroda, K. Uchino, Y. Hasegawa, S. Morooka, *AIChE J.* 45 (1999) 1220.
- [17] K. Kusakabe, T. Kuroda, S. Morooka, *J. Membr. Sci.* 148 (1998) 13.
- [18] C.D. Baertsch, H.H. Funke, J.L. Falconer, R.D. Noble, *J. Phys. Chem.* 100 (1996) 7676.
- [19] G. Bonilla, M. Tsapatsis, D.G. Vlachos, G. Xomeritakis, *J. Membr. Sci.* 182 (2001) 103.
- [20] W.S. Dai, T.A. Barbari, *J. Membr. Sci.* 171 (2000) 45.
- [21] C. Charcosset, J.-C. Bernengo, *J. Membr. Sci.* 168 (2000) 53.
- [22] V. Nikolakis, G. Xomeritakis, A. Abibi, M. Dickson, M. Tsapatsis, D.G. Vlachos, *J. Membr. Sci.* 184 (2001) 209.
- [23] J.P.G. Villaluenga, A. Tabe-Mohammadi, *J. Membr. Sci.* 169 (2000) 159.
- [24] J.L. Humphrey, G.E. Keller, *Separation Process Technology*, McGraw-Hill, New York, 1997.
- [25] Y. Lu, R. Ganguli, C.A. Drewien, M.T. Anderson, C.J. Brinker, W. Gong, Y. Guo, H. Soyez, B. Dunn, M.H. Huang, J.I. Zink, *Nature* 389 (1997) 364.
- [26] G. Xomeritakis, Z. Lai, M. Tsapatsis, *Ind. Engng. Chem. Res.* 40 (2001) 544.
- [27] B.J. Schoeman, J. Sterte, J.E. Otterstedt, *J. Colloid Interf. Sci.* 170 (1995) 449.
- [28] S. Qiu, J. Yu, G. Zhu, O. Terasaki, Y. Nozue, W. Pang, R. Xu, *Micropor. Mesopor. Mater.* 21 (1998) 245.
- [29] D. Barthomeuf, B.H. Ha, *J. Chem. Soc. Faraday Trans.* (1973) 2147.